

Interpreting the Observed Clustering of Red Galaxies at $z \sim 3$

Zheng Zheng

Department of Astronomy, Ohio State University, Columbus, OH 43210, USA

zhengz@astronomy.ohio-state.edu

ABSTRACT

Daddi et al. have recently reported strong clustering of a population of red galaxies at $z \sim 3$ in the Hubble Deep Field–South. Fitting the observed angular clustering with a power law of index -0.8 , they infer a comoving correlation length $r_0 \sim 8h^{-1}\text{Mpc}$; for a standard cosmology, this r_0 would imply that the red galaxies reside in rare, $M \geq 10^{13}h^{-1}M_\odot$ halos, with each halo hosting ~ 100 galaxies to match the number density of the population. Using the framework of the halo occupation distribution (HOD) in a ΛCDM universe, we show that the Daddi et al. data can be adequately reproduced by less surprising models, e.g., models with galaxies residing in halos of mass $M > M_{\text{min}} = 6.3 \times 10^{11}h^{-1}M_\odot$ and a mean occupation $N_{\text{avg}}(M) = 1.4(M/M_{\text{min}})^{0.45}$ above this cutoff. The resultant correlation functions do not follow a strict power law, showing instead a clear transition from the one-halo–dominated regime, where the two galaxies of each pair reside in the same dark matter halo, to the two-halo–dominated regime, where the two galaxies of each pair are from different halos. The observed high-amplitude data points lie in the one-halo–dominated regime, so these HOD models are able to explain the observations despite having smaller correlation lengths, $r_0 \sim 5h^{-1}\text{Mpc}$. HOD parameters are only loosely constrained by the current data because of large sample variance and the lack of clustering information on scales that probe the two-halo regime. If our explanation of the data is correct, then future observations covering a larger area should show that the large scale correlations lie below a $\theta^{-1.8}$ extrapolation of the small scale points. Our models of the current data suggest that the red galaxies are somewhat more strongly clustered than UV-selected Lyman-break galaxies and have a greater tendency to reside in small groups.

Subject headings: galaxies: halos – galaxies: high-redshift – large-scale structure of universe

1. Introduction

Clustering of high-redshift galaxies can provide information about their relation to the underlying mass distribution and their formation mechanisms. Efforts have been made to detect high- z

galaxies and to estimate their clustering properties. For example, surveys of $z \sim 3$ Lyman break galaxies (LBGs) (Adelberger et al. 1998, 2003; Steidel et al. 1998) show that these galaxies are strongly clustered, with a correlation length $r_0 \sim 4h^{-1}\text{Mpc}$. This strong clustering appears to be naturally explained by theoretical models, which predict high bias of luminous high- z galaxies (Governato et al. 1998; Kauffmann et al. 1999; Cen & Ostriker 2000; Benson et al. 2001; Pearce et al. 2001; Somerville et al. 2001; Yoshikawa et al. 2001; Weinberg et al. 2004). Recently, using VLT observations, Daddi et al. (2003) have analyzed the clustering properties of $K \leq 24$ galaxies in the Hubble Deep Field South (HDF-S). They find that a population of red galaxies with $J - K > 1.7$ in the photometric redshift range $2 < z_{\text{phot}} < 4$ exhibit remarkably strong clustering, $r_0 \sim 8h^{-1}\text{Mpc}$. This paper attempts to interpret these measurements in the framework of halo occupation distribution (HOD) models (see, e.g., Seljak 2000; Scoccimarro et al. 2001; Berlind & Weinberg 2002 and references therein).

Fitting the measured two-point angular correlation function by a power law with an index -0.8 , which corresponds to a power law real-space two-point correlation function with an index -1.8 , Daddi et al. (2003) derive a correlation length as large as $r_0 \sim 8h^{-1}\text{Mpc}$ for the red galaxies. This strong clustering seems hard to reconcile with conventional models of galaxy bias. For a reasonable cosmological model, such as that assumed in the GIF simulation of Jenkins et al. (1998), a correlation length of $\sim 8h^{-1}\text{Mpc}$ corresponds to a linear galaxy bias factor of ~ 5 at $z \sim 3$. In the halo bias model (e.g. Mo & White 1996), this bias factor implies that these red galaxies would be hosted by $M \geq 10^{13}M_{\odot}$ halos. The comoving number density of $M \geq 10^{13}M_{\odot}$ halos is $\sim 3 \times 10^{-5}h^3\text{Mpc}^{-3}$. To match the comoving number density, $\sim 7 \times 10^{-3}h^3\text{Mpc}^{-3}$, of the red galaxies, there should be more than 200 such galaxies in each halo. Even if we take into account the fact that galaxy bias is an average of halo bias weighted by occupation numbers and lower the halo mass to $M \geq 5 \times 10^{12}M_{\odot}$, the occupation number is still as large as about 70. Based on the data, Daddi et al. (2003) speculate that the problem may be caused by the effect of a small scale excess in the correlation function. Detailed modeling is necessary to resolve this puzzle.

For modeling observed galaxy clustering statistics, the framework of the HOD is a powerful tool. The HOD describes the relation between the distribution of galaxies and that of the matter at the level of individual dark matter halos. It characterizes the probability distribution $P(N|M)$ that a halo of mass M contains N galaxies of a given type and specifies the relative spatial and velocity distributions of galaxies and dark matter within halos. With an assumed cosmological model that determines the halo population, the HOD can be inferred empirically from observed galaxy clustering (Peacock & Smith 2000; Marinoni & Hudson 2002; Berlind & Weinberg 2002). HOD modeling has been applied to galaxy clustering data from the Two-Degree Field Galaxy Redshift Survey (2dFGRS) and the Sloan Digital Sky Survey (SDSS) (see, e.g., van den Bosch et al. 2003; Magliocchetti & Porciani 2003; Zehavi et al. 2004). HOD modeling has also been used to model the clustering of high- z galaxies, such as LBGs (Bullock, Wechsler, & Somerville 2002) and extremely red objects (EROs) (Moustakas & Somerville 2002).

In this paper, we will apply HOD modeling to the population of red galaxies at $z \sim 3$ in Daddi

et al. (2003) and try to understand the apparent strong clustering of these galaxies. We describe the HOD parameterization and how we analytically calculate the galaxy correlation function in § 2. In § 3, we explain what we learn from model fitting to the observational data. We summarize the results and give a brief discussion in § 4.

2. HOD Parameterization and Analytic Calculation of Correlation Function

Motivated by measurements of the cosmic microwave background (e.g., Netterfield et al. 2002; Pryke et al. 2002; Spergel et al. 2003), the abundance of galaxy clusters (e.g., Eke, Cole, & Frenk 1996), and high redshift supernova observations (e.g., Riess et al. 1998; Perlmutter et al. 1999), we adopt a spatially flat Λ CDM cosmological model with matter density parameter $\Omega_m = 0.3$ throughout this paper. For the matter fluctuation power spectrum, we adopt the parameterization of Efstathiou, Bond, & White (1992) and assume that the spectral index of the inflationary power spectrum is $n_s = 1$, the rms fluctuation (linearly evolved to $z = 0$) at a scale of $8h^{-1}\text{Mpc}$ is $\sigma_8 = 0.9$, and the shape parameter is $\Gamma = 0.21$. The Hubble constant is assumed to be $100h \text{ km s}^{-1} \text{ Mpc}^{-1}$ with $h = 0.7$.

2.1. HOD parameterization

To do an analytical calculation of the correlation function of galaxies, we need to parameterize the halo occupation distribution. For the functional form of halo occupation number, we adopt a simple model similar to that used by Zehavi et al. (2004), which is loosely motivated by results from smoothed particle hydrodynamics (SPH) simulations and semi-analytic calculations (see Berlind et al. 2003 and references therein). In this model, in halos of mass $M \geq M_1$, the mean occupation number follows a power law, $N_{\text{avg}}(M) = (M/M_1)^\alpha$, and in halos of mass $M_{\text{min}} \leq M < M_1$ there is only a single galaxy that is above the luminosity threshold, i.e., $N_{\text{avg}}(M) = 1$. Given α and M_1 , M_{min} is then fully determined by the number density of galaxies. Since the correlation function is a statistic of galaxy pairs, we also need to know the second moment of the occupation number. SPH simulations and semi-analytic models predict that the distribution of halo occupation numbers at fixed halo mass is much narrower than a Poisson distribution when the occupation is low. Here we adopt the so-called nearest-integer distribution for $P(N|N_{\text{avg}})$, which states that the occupation number for a halo of mass M is one of the two integers bracketing $N_{\text{avg}}(M)$, with the relative probability determined by having the right mean. Besides this basic model, we will also consider some alternatives as discussed in § 3. More detailed discussions of the parameterization of HOD models appear in Berlind et al. (2003) and Zehavi et al. (2004). Our parameterization here is quite restrictive, but the data are not sufficient to constrain a model with more freedom.

2.2. Real Space Correlation Function

The two-point correlation function of galaxies $\xi(r)$ reflects the excess probability over a random distribution of finding galaxy pairs with a separation r . From the point view of the halo model, the two galaxies of each pair can come from either a single halo or two different halos. Consequently, the two-point correlation function $\xi(r)$ can be decomposed into two components,

$$\xi(r) = [1 + \xi_{1h}(r)] + \xi_{2h}(r), \quad (1)$$

where the one-halo term $\xi_{1h}(r)$ and the two-halo term $\xi_{2h}(r)$ represent contributions by pairs from single halos and different halos, respectively. The above expression comes from the fact that the total number of galaxy pairs ($\propto 1 + \xi(r)$) is simply the sum of the number of pairs from single halos ($\propto 1 + \xi_{1h}(r)$) and that from different halos ($\propto 1 + \xi_{2h}(r)$). The one-halo term and two-halo term dominate respectively at small and large separations.

The one-halo term $\xi_{1h}(r)$ can be exactly computed in real space through (Berlind & Weinberg 2002)

$$1 + \xi_{1h}(r) = \frac{1}{2\pi r^2 \bar{n}_g^2} \int_0^\infty dM \frac{dn}{dM} \frac{\langle N(N-1) \rangle_M}{2} \frac{1}{2R_{\text{vir}}(M)} F' \left(\frac{r}{2R_{\text{vir}}} \right), \quad (2)$$

where \bar{n}_g is the mean number density of galaxies, dn/dM is the halo mass function (Sheth & Tormen 1999; Jenkins et al. 2001), $\langle N(N-1) \rangle_M/2$ is the average number of pairs in a halo of mass M , and $F(r/2R_{\text{vir}})$ is the cumulative radial distribution of galaxy pairs, i.e. the average fraction of galaxy pairs in a halo of mass M (virial radius R_{vir}) that have separation less than r . The function $F'(x)$ depends on the profile of the galaxy distribution $\rho_g(r)$ within the halo. In this paper, we assume that there is always a galaxy located at the center of the halo, and others are regarded as satellite galaxies. With this assumption of central galaxies, $F'(x)$ is then the pair-number weighted average of the central-satellite pair distribution $F'_{\text{cs}}(x)$ and the satellite-satellite pair distribution $F'_{\text{ss}}(x)$ (see, e.g., Berlind & Weinberg 2002; Yang, Mo, & van den Bosch 2002),

$$\frac{\langle N(N-1) \rangle_M}{2} F'(x) = \langle N-1 \rangle_M F'_{\text{cs}}(x) + \frac{\langle (N-1)(N-2) \rangle_M}{2} F'_{\text{ss}}(x). \quad (3)$$

The central-satellite galaxy pair distribution $F'_{\text{cs}}(x)$ is just the normalized radial distribution of galaxies (i.e., $\propto \rho_g(r)r^2$), and the satellite-satellite galaxy pair distribution $F'_{\text{ss}}(x)$ can be derived through the convolution of the galaxy distribution profile with itself (see Sheth et al. 2001). We will first assume that the galaxy distribution is the same as the dark matter distribution within the halo, which follows an NFW profile (Navarro, Frenk, & White 1995, 1996, 1997) truncated at the virial radius. The concentration of an NFW profile depends on the halo mass, for which we use the relation given by Bullock et al. (2001) after modifying it to be consistent with our halo definition – a gravitationally bound structure with overdensity ~ 200 . Later in this paper, we will also consider a more concentrated galaxy distribution profile.

The two-halo term is basically the average halo correlation function weighted by the average occupation number of galaxies of each halo. The halo correlation function is related to the mass

correlation function by the halo bias factor (Mo & White 1996; Jing 1998; Sheth, Mo, & Tormen 2001). It is convenient to calculate the two-halo term in Fourier space (Seljak 2000; Scoccimarro et al. 2001). The two-halo term contribution to the galaxy power spectrum reads

$$P_{\text{gg}}^{2\text{h}}(k) = P_m(k) \left[\frac{1}{\bar{n}_g} \int_0^{M_{\text{max}}} dM \frac{dn}{dM} N_{\text{avg}}(M) b_h(M) y_g(k, M) \right]^2, \quad (4)$$

where $P_m(k)$ is the mass power spectrum, $N_{\text{avg}}(M)$ is the mean occupation number in halos of mass M , $b_h(M)$ is the halo bias factor, $y_g(k, M)$ is the (normalized) Fourier transform of the galaxy distribution profile within a halo of mass M , and M_{max} is the upper limit for the integral (see below). In the calculation, we adopt the three improvements mentioned in Zehavi et al. (2004). First, for $P_m(k)$, instead of the linear spectrum as used in previous studies, we use the non-linear power spectrum as given by Smith et al. (2003) to account for the non-linear evolution of the mass (also see Magliocchetti & Porciani 2003). Second, the halo exclusion effect is approximately considered by choosing an appropriate M_{max} : for the two-halo term at separation r , M_{max} is taken to be the mass of the halo with virial radius $r/2$. Third, the scale-dependence of the halo bias factor on non-linear scales is incorporated by using an empirical formula from simulations. The two-halo term of the correlation function is the Fourier transform of the power spectrum,

$$\xi_{2\text{h}}(r) = \frac{1}{2\pi^2} \int_0^\infty P_{\text{gg}}^{2\text{h}}(k) k^2 \frac{\sin kr}{kr} dk. \quad (5)$$

The correlation function analytically calculated using the above method agrees fairly well with that measured from a mock galaxy catalog generated by populating galaxies according to the same HOD into halos identified in N -body simulations (see Zehavi et al. 2004 and Figure 2 below).

2.3. Angular Correlation Function

The angular distribution of galaxies is a projection of the three-dimensional distribution. The angular correlation function $w(\theta)$ of galaxies is related to the real-space correlation function through Limber's equation (Peebles 1980). In a flat universe, as adopted in this paper, for the small-angle limit, Limber's equation has the form

$$w(\theta) = \frac{\int_{r_{\text{min}}}^{r_{\text{max}}} \bar{n}_g^2(x) S^2(x) x^4 dx \int_{-\Delta r}^{\Delta r} \xi(\sqrt{y^2 + x^2 \theta^2}, z) dy}{\left[\int_{r_{\text{min}}}^{r_{\text{max}}} \bar{n}_g(x) S(x) x^2 dx \right]^2}, \quad (6)$$

where $\Delta r = r_{\text{max}} - r_{\text{min}}$ is the radial range of the survey, $\bar{n}_g(r)$ is the average number density of galaxies at distance r , and $S(r)$ is the selection function of the sample (all distances are in comoving units). The sample selection function $S(r)$ can be derived from the observed redshift distribution if the sample is large enough, but the 49 galaxy sample of Daddi et al. (2003) is not large enough to allow a precise measurement. However, it turns out that the basic result of this paper is not

sensitive to the form of the selection function. We therefore simply assume that $S(r)$ is constant over the redshift range $z = 2$ to $z = 4$, which defines r_{\min} and r_{\max} .

In practice, the angular correlation function is estimated by comparing the observed pair numbers in an angular separation bin with those from a random sample of the same geometry. The widely used estimator proposed by Landy & Szalay (1993) estimates the angular correlation function as

$$w_b(\theta) = \frac{\text{DD} - 2\text{DR} + \text{RR}}{\text{RR}}, \quad (7)$$

where DD, DR, and RR represent number counts of data-data (galaxy-galaxy) pairs, data-random (galaxy-random) pairs, and random-random pairs, respectively, in the angular bin around θ . Each of these number counts are normalized so that the summation over all θ is unity (i.e., the number of pairs in each angular bin is divided by the total number of pairs in the field). The estimated angular correlation function $w_b(\theta)$ is subject to a statistical bias that leads to systematically lower values than the true angular correlation function $w(\theta)$, $w_b(\theta) = w(\theta) - I.C.$, where

$$I.C. = \frac{1}{\Omega^2} \int \int w(\theta) d\Omega_1 d\Omega_2 \quad (8)$$

is the integral constraint (Groth & Peebles 1977). Since $w_b(\theta)$ is the quantity directly measured from the observation, it is more appropriate to try to fit $w_b(\theta)$ than to fit $w(\theta)$. To convert the analytically predicted $w(\theta)$ to $w_b(\theta)$, we use the random-random sample to calculate the integral constraint expected for the model $w(\theta)$ (see, e.g., Roche et al. 1999),

$$I.C. = \frac{\sum N_{\text{rr}}(\theta)w(\theta)}{\sum N_{\text{rr}}(\theta)}, \quad (9)$$

where $N_{\text{rr}}(\theta)$ is the count of random-random pairs in the angular bin around θ . We only need to estimate $f(\theta) = N_{\text{rr}}(\theta)/\sum N_{\text{rr}}(\theta)$ once from a random sample that has the same geometry as the observation. We generate 100 such random samples with 5,000 points in each and take the average $f(\theta)$ as the estimate.

3. Fitting the Observations

The angular clustering data we are interested in are for a population of K -selected galaxies ($K \leq 24$) at $2 < z_{\text{phot}} < 4$ with $J - K > 1.7$. Details about this sample can be found in Daddi et al. (2003). The sample includes 49 galaxies found within a field of view of ~ 4 arcmin². The comoving number density of these galaxies is $\sim 7.1 \times 10^{-3} h^3 \text{Mpc}^{-3}$. Assuming the angular correlation function to be a power law with an index -0.8 , Daddi et al. (2003) find its amplitude at 1° to be 39.1 ± 10.2 , which corresponds to a real space correlation length of $8.3 \pm 1.2 h^{-1} \text{Mpc}$ (comoving).

We now fit the data (kindly provided in electronic form by E. Daddi) using the model in § 2. For a given assumption about $P(N|N_{\text{avg}})$, e.g., a nearest-integer or Poisson distribution, the analytic angular correlation model discussed in § 2.3 has two free parameters: M_1 , which determines the

amplitude of $N_{\text{avg}}(M)$, and α , which is the slope of $N_{\text{avg}}(M)$ at high halo masses. M_{min} is fixed by the mean number density of galaxies in the sample. We thus perform a two-parameter χ^2 fit to the data. The observational error bars reported by Daddi et al. (2003) are used in the calculation of χ^2 and are assumed to be uncorrelated. With these data and error bars, we find that the two free HOD parameters are highly degenerate and that they can be only loosely constrained individually. For example, with the nearest-integer distribution, M_1 is in the range $4\text{--}30 \times 10^{10} h^{-1} M_{\odot}$ and α is in the range 0.2–0.5. If we assume a Poisson distribution for $P(N|N_{\text{avg}})$, then the resultant α is unrealistically large (~ 3), with large uncertainty. With the Poisson distribution, if we change the functional form of $N_{\text{avg}}(M)$ to be a power law with a low mass cutoff, α can be in a reasonable range but still with large uncertainty. Through studying subhalos in high-resolution dissipationless simulations, Kravtsov et al. (2004) propose an HOD form, which separates contributions from central and satellite galaxies. The mean occupation function of central galaxies is a step function, while the distribution of satellite galaxies can be approximated by a Poisson distribution with the mean following a power law. The resultant shape of the mean occupation function and scatter around the mean are somewhat similar to our basic model. We also try this HOD form and find results and uncertainties similar to those of our basic model.

We illustrate the looseness of the HOD parameter constraints in Figure 1 by showing the results of different parameter combinations that lead to similar real-space correlations and angular correlations for the nearest-integer case. Note that since $M_{\text{min}} > M_1$ is derived from the fit, the resultant $N_{\text{avg}}(M)$ is equivalent to a case in which $N_{\text{avg}}(M)$ is a power law with a low-mass cutoff, with no “flat” portion at $M < M_1$. The result of $M_{\text{min}} > M_1$ mimics the case of local giant elliptical galaxies and $z \sim 1$ EROs as modeled by Moustakas & Somerville (2002), a point discussed further at the end of this section. There is a strong break in the modeled correlation function between the one-halo and two-halo regimes. The sharpness of this break is somewhat exaggerated by the approximate nature of our correction for halo exclusion. However, the angular correlation function is less affected by this approximation because it is a projection of the real-space correlation, and we show later that the approximate treatment of halo exclusion has a negligible effect on our $w_b(\theta)$ modeling here.

The reduced χ^2 (7 degrees of freedom, 9 data points, and 2 free parameters) from either the nearest-integer model or the power law Poisson model is about 1.8, which does not seem to be a good model fit. The field of view of the survey is less than 4 arcmin², and the total number of galaxies is only about 50. Thus, as noted by Daddi et al. (2003), the sample variance may be large, and error bars based only on the finite number of objects (as used above) may be too small. We therefore attempt to make more realistic error estimates by populating halos from the GIF simulation (Jenkins et al. 1998) with galaxies. We use the halo population from the GIF simulation output at $z = 2.97$ and proceed as follows. First, each halo is assumed to have a truncated NFW density profile with the same concentration-mass relation used in the analytic model. We then populate galaxies according to the halo occupation distribution from the χ^2 fitting and generate a mock galaxy catalog. Next, we randomly extract 10 slices along one direction from the mock

catalog, with the cross-section of each slice having the same size and geometry as the observation. These 10 slices are checked at selection to make sure that they do not overlap (even partially) with each other. The 10 slices are stacked together to approximate the radial extent of the survey in comoving distance. The projection of the stacked slice thus represents one “observation.” Finally, we estimate $w_b(\theta)$ for this observation in the same angular bins as the real data using the technique of Landy & Szalay (1993) (Equation 7). The data-random and random-random terms are averaged over 100 random realizations, and each random sample realization has 5000 points. Altogether we make 100 observations and estimate $w_b(\theta)$ for each one.

The result is shown in the top left panel of Figure 2. The central solid line is the average over the 100 observations, which agrees with the model prediction (*dot-dashed line*) as expected (and verifying that our analytic approximation is accurate enough for our purposes). The dashed lines above and below the solid line represent the 1σ scatter of the 100 observations. The estimated angular correlation $w_b(\theta)$ for an individual observation is very uncertain and may even not decrease monotonically with θ (as is the case for the real data points). Compared with the scatter derived here, the observational error bars are apparently underestimated by a factor of about 1.5. If we take the mock catalog scatter as true error bars, then our model fit is acceptable. However, the uncertainties in HOD parameters were large even with the original error bars, so we do not wish to place much weight on the particular values that emerge in the best fit. Rather, we wish to use our HOD models as a general guide in understanding the implications of the data. Perhaps the most important lesson is that the observed angular correlation signals are dominated by the one-halo term, where the two galaxies of each pair are from one single halo. This can be seen in the top left panel of Figure 2, where the dotted line shows the two-halo term. The contribution from the two halo term becomes comparable to that from the one-halo term only on angular scales greater than $\sim 0''.005$ (also see the bottom left panel of Figure 1). As mentioned in Daddi et al. (2003), the estimated angular correlation at the smallest angular scale is mainly from a few triplets. The redshift distribution of the galaxy sample provides further evidence. There are many spiky structures in the redshift distribution (Daddi et al. 2003). Since the largest projected separation in the field of view is about $3h^{-1}\text{Mpc}$, galaxies within the same spike are most likely to be physically close, and thus they have a high probability of being located in the same halo.

Domination of the signal by the one-halo term has several implications. The HOD model generically predicts that the correlation function is not strictly a power law (see Berlind & Weinberg 2002). Instead, there should be a transition region from the one-halo-dominated regime at small scales to the two-halo-dominated regime at large scales. For the real-space correlation function, such a transition happens around the virial radius of the largest halos, $2 - 3h^{-1}\text{Mpc}$ at $z = 0$. Recent results from SDSS have revealed a statistically significant departure from a power law in the two-point correlation function, which can be well explained within the framework of the HOD (Zehavi et al. 2004). Two-point correlation functions measured from other surveys, such as 2dFGRS and APM, also show such a departure (e.g. Hawkins et al. 2003; Padilla & Baugh 2003).

The two-point correlation function predicted by the model that fits the angular correlation

function in this paper shows a prominent departure from a power law (Figures 1 and 2), which is also reflected in the predicted angular correlation function (Figure 1). [Note that the excellent agreement between the numerical and analytic calculations of $w_b(\theta)$ demonstrates that any artifacts of our approximate treatment of halo exclusion are negligible in comparison to the observational error bars.] Since the one-halo term is related to the distribution of galaxies within halos and the two-halo term is mostly determined by the halo-halo distribution, the amplitude and slope of the two terms may differ from each other substantially. One should therefore be cautious about inferring the correlation length by assuming a pure power law in the correlation function. In Daddi et al. (2003), a power law with an index -1.8 for the real-space correlation function, corresponding to an index of -0.8 for the angular correlation function, is assumed, and a high correlation amplitude (correlation length $\sim 8h^{-1}\text{Mpc}$) is found. This strong correlation is unlikely to be related to the real correlation between halos, since, as we show here, the statistically significant signal is dominated by galaxy pairs within halos. The distribution of galaxies within halos does not tell how galaxies cluster on large scales, and the correlation length is overestimated because of the high amplitude of the one-halo term. In fact, from the fitting model, the correlation length where $\xi(r) = 1$ can be as low as $\sim 5h^{-1}\text{Mpc}$ (Figure 2), which is in a good agreement with the result of Kravtsov et al. (2004) for a subhalo sample of comparable number density. The mystery about the strong clustering in this particular sample then disappears. Our explanation of this mystery is, in some sense, a quantitative version of the speculation of Daddi et al. (2003) that the strong clustering signal is an effect of “excess” small-scale clustering.

We note that although the fit to the data can be regarded as acceptable, the third and the fourth data points are well below the prediction. This may be of no significance considering the large sample variance. Nevertheless, it is interesting to ask what the cause may be if this discrepancy is real. The low amplitude of these two data points may be a hint that the one-halo term drops faster than in our model, which means that the distribution of galaxies within halos is more concentrated than the NFW profile we use. As an alternative model, we first doubled the concentration parameter of the galaxy distribution profile within each halo, thus making the galaxies more centrally concentrated than the dark matter, but this change is not adequate to match the observed $w_b(\theta)$ in the third and fourth angular bins. It thus implies that the distribution profile of galaxies is steeper than the NFW profile. As a more extreme alternative, we considered an r^{-3} profile, with a flat core at $r < 0.1R_{\text{vir}}$ to make the pair distribution finite. The bottom panels of Figure 2 show the resultant model fitting and the sample variance estimated from mock catalogs generated using halos in the GIF simulation. The steeper galaxy distribution yields a better fit to the third and fourth data points. As before, HOD parameters remain poorly constrained. With the current sample size, the preference for r^{-3} profiles over NFW profiles is not highly significant, but the low amplitude of the third and fourth data points could be a hint that the red galaxies in the sample of Daddi et al. (2003) are centrally concentrated within their parent halos, analogous to the morphological segregation observed in present-day clusters (e.g., Oemler 1974; Melnick & Sargent 1977; Dressler 1980; Adami, Biviano, & Mazure 1998).

Although HOD parameters are loosely constrained, the cutoff mass M_{\min} in all the models shown in the figures roughly remains constant, $\sim 6 \times 10^{11} h^{-1} M_{\odot}$. The approximate constancy of M_{\min} mainly comes from the constraint of the galaxy number density and the steep drop of the halo number density toward higher halo masses. For example, the cumulative number density of halos drops from $\sim 5 \times 10^{-3} h^3 \text{Mpc}^{-3}$ to $\sim 3 \times 10^{-3} h^3 \text{Mpc}^{-3}$ as the minimum halo mass changes from $5 \times 10^{11} h^{-1} M_{\odot}$ to $7 \times 10^{11} h^{-1} M_{\odot}$. With the galaxy number density fixed, a large change in M_{\min} is hard to compensate with changes in other HOD parameters. Although the sharp cutoff in $N_{\text{avg}}(M)$ that we have assumed in this paper is an idealization, the derived value of M_{\min} should still give an approximate indication of the characteristic minimum masses of halos that host the red galaxies. In our successful models, the mean occupation number at M_{\min} is above 1 (i.e., $M_{\min} > M_1$). This suggests that the red galaxies arise preferentially in groups and clusters (see Moustakas & Somerville 2002), which may be a signature of an environmental effect on color. However, since $M_{\min} < M_2$, where M_2 is the mass of the halo that on average contains two red galaxies, there are still single-occupancy halos as the nearest-integer distribution is taken into account. For example, in the model with $\alpha = 0.45$ and $M_{\min} = 6.3 \times 10^{11} h^{-1} M_{\odot}$, $M_2 = 1.4 \times 10^{12} h^{-1} M_{\odot}$, and about 11% of the galaxies are the sole occupants of their halos.

There are several hints that the red galaxies of the Daddi et al. (2003) sample have clustering properties different from those of the UV-selected galaxies (e.g., LBGs) at the same redshift. The first hint comes from the $M_{\min} > M_1$ result mentioned above. Using similar kinds of HOD models (although assuming a pure power law with a low mass cutoff, with no single occupancy “plateau”), Bullock, Wechsler, & Somerville (2002) and Moustakas & Somerville (2002) find $M_{\min} \sim 10^{10} h^{-1} M_{\odot} \ll M_1$ for LBGs at $z \sim 3$, implying that most LBGs are the sole occupants of their parent halos. By contrast, our model fits imply that most red galaxies reside in groups of two or more, similar to the results of Moustakas & Somerville (2002) for local giant elliptical galaxies and $z \sim 1$ EROs (for which they find a trend of $M_{\min} > M_1$). A second hint is from the correlation length itself, which is still $\sim 5 h^{-1} \text{Mpc}$ in our models. The correlation length of UV-selected LBGs in the spectroscopic sample of Adelberger et al. (2003) is only about $4 h^{-1} \text{Mpc}$, and it appears to decrease for samples of lower luminosity threshold and higher space density (Giavalisco & Dickinson 2001). A final hint comes from the behavior of clustering on small scales. Porciani & Giavalisco (2002) find that the angular correlation function of $z \sim 3$ LBGs drops at separations of less than $30''$, while the angular clustering of the red galaxies seems, if anything, to be exceptionally strong at the smallest angular scales. To illustrate these differences between the red galaxies and the UV-selected LBGs, we show in Figure 1 what the HOD and correlation functions would look like for an LBG sample that has the same number density as the red galaxies. For this purpose, we start from the HOD model result of $z \sim 3$ LBGs by Moustakas & Somerville (2002), which is consistent with that of Bullock, Wechsler, & Somerville (2002), and change their HOD parameters a little bit to match the number density here. The mean occupation function has a power-law form $N_{\text{avg}}(M) = (M/M_1)^{\alpha}$ with a low-mass cutoff M_{\min} . We adopt $M_{\min} = 1.4 \times 10^{10} h^{-1} M_{\odot}$, $M_1 = 4.0 \times 10^{12} h^{-1} M_{\odot}$, $\alpha = 0.8$, and a nearest-integer distribution. The dashed line in the top right panel of Figure 1 shows this mean occupation function, where we can clearly see that unlike

the red galaxies, relatively fewer LBGs reside in groups. This leads to a lower small-scale clustering amplitude and a lower correlation length with respect to the red galaxies (see the dashed curves in the left panels of Figure 1). For a more consistent comparison between the red galaxies and the LBGs, we need detailed HOD modeling of the LBGs, which is out of the scope of this paper. The exercise here is to simply illustrate the differences in the clustering properties of the red galaxies and the LBGs, as noticed by Roche et al. (2002), Roche, Dunlop, & Almaini (2003), and Daddi et al. (2003) from angular clustering measurements.

4. Conclusion and Discussion

In this paper, we have presented an HOD model of the observed strong clustering of a population of red galaxies at $z \sim 3$ analyzed by Daddi et al. (2003). Fitting the angular correlation data by assuming the real-space correlation to be a power law with the form $(r/r_0)^{-1.8}$, Daddi et al. (2003) find the correlation length $r_0 \sim 8h^{-1}\text{Mpc}$, which would imply that galaxies reside in rare halos with $M \geq 10^{13}h^{-1}M_\odot$ and which would require a very large occupation number in each halo to account for the observed galaxy number density. Our HOD modeling shows that the angular clustering data can be explained by a less surprising model, e.g., with a cutoff at $6.3 \times 10^{11}h^{-1}M_\odot$ and mean galaxy occupation number $N_{\text{avg}}(M) = 1.4(M/6.3 \times 10^{11}h^{-1}M_\odot)^{0.45}$ above this cutoff. Artificial galaxy catalogs constructed with this HOD show that sample variance increases error bars by $\sim 50\%$ over those estimated by Daddi et al. (2003), which (as they noted) did not take sample variance into account.

There is degeneracy between HOD parameters M_1 and α . However, the characteristic minimum mass of halos that can host the red galaxies seems to be around $6 \times 10^{11}h^{-1}M_\odot$. Results from our modeling suggest that the red galaxies are a different population from LBGs.

HOD parameters are not tightly constrained by the data, but in all cases the significantly non-zero points from Daddi et al. (2003) are in a regime dominated by pairs within single halos. The amplitude of the correlation function in the two-halo regime is below an $r^{-1.8}$ power law extrapolation of that of the one-halo regime, which is why lower mass halos are acceptable. Thus, if our explanation is correct, surveys with larger area should show weaker correlations than this $r^{-1.8}$ extrapolation. The correlation length predicted by our model can be as low as $\sim 5h^{-1}\text{Mpc}$, a prediction that can be tested by larger area surveys.

Obtaining good constraints on HOD parameters will require samples large enough to accurately probe the two-halo regime as well as the one-halo regime. Spectroscopic surveys are also of importance since they allow one to measure galaxy clustering in redshift space (in addition to more accurate measurements of the projected clustering). With a good understanding of the velocity field of halos, the clustering in redshift space would at least provide a consistency check for the HOD

model. With wider angle space-based surveys such as GOODS¹ and ambitious infrared follow-up programs like the FIRES project (Franx et al. 2000; Daddi et al. 2003), the necessary data should become available in the next several years. This will provide valuable constraints on the host halos of red high- z galaxies and clues to their formation histories.

We thank Emanuele Daddi not only for providing us the observation geometry and the angular clustering data used in this paper but also for his useful comments and suggestions. We also thank David Weinberg for helpful discussions, for his encouragement on this work, and for his valuable comments that improved the paper. This work was supported by NSF grant AST 00-98584 and by a Presidential Fellowship from the Graduate School of the Ohio State University.

REFERENCES

- Adami, C., Biviano, A., & Mazure, A. 1998, *A&A*, 331, 439
- Adelberger, K. L., Steidel, C. C., Giavalisco, M., Dickinson, M., Pettini, M., Kellogg, M. 1998, *ApJ*, 505, 18
- Adelberger, K. L., Steidel, C. C., Shapley, A. E., & Pettini, M. 2003, *ApJ*, 584, 45
- Benson, A. J., Frenk, C. S., Baugh, C. M., Cole, S., & Lacey, C. G. 2001, *MNRAS*, 327, 1041
- Berlind, A. A., & Weinberg, D. H. 2002, *ApJ*, 575, 587
- Berlind, A. A., Weinberg, D. H., Benson, A. J., Baugh, C. M., Cole, S., et al. 2003, *ApJ*, 593, 1
- Bullock, J. S., Kolatt, T. S., Sigad, Y., Somerville, R. S., Klypin, A. A., Primack, J. R., Dekel, A. 2001, *MNRAS*, 321, 559
- Bullock, J. S., Wechsler, R. H., & Somerville, Rachel, S. 2002, *MNRAS*, 329, 246
- Cen, R., & Ostriker, J. P. 2000, *ApJ*, 538, 83
- Daddi, E., Röttgering, H. J. A., Labbé, I., Rudnick, G., et al. 2003, *ApJ*, 588, 50
- Dressler, A. 1980, *ApJ*, 236, 351
- Efstathiou, G., Bond, J. R., & White, S. D. M. 1992, *MNRAS*, 258, 1
- Eke, V. R., Cole, S., & Frenk, C. S. 1996, *MNRAS*, 282, 263
- Franx, M., et al. 2000, *ESO Messenger*, 99 20

¹See <http://www.stsci.edu/science/goods>.

- Giavalisco, M. G., & Dickinson, M. 2001, *ApJ*, 550, 177
- Governato, F., Baugh, C. M., Frenk, C. S., Cole, S., Lacey, C. G., Quinn, T. R., & Stadel, J. 1998, *Nature*, 392, 359
- Groth, E. J., & Peebles, P. J. E. 1977, *ApJ*, 217, 38
- Hawkins, E., Maddox, S., Cole, S., Madgwick, D., Norberg, P., et al. 2002, *MNRAS*, 346, 78
- Jenkins, A., Frenk, C. S., Pearce, F. R., Thomas, P. A., Colberg, J. M., White, S. D. M., Couchman, H. M. P., Peacock, J. A., & Efstathiou, G., & Nelson, A. H. 1998, *ApJ*, 499, 20
- Jenkins, A., Frenk, C. S., White, S. D. M., Colberg, J. M., Cole, S., Evrard, A. E., Couchman, H. M. P., & Yoshida, N. 2001, *MNRAS*, 321, 372
- Jing, Y. P. 1998, *ApJ*, 503, L9
- Kauffmann, G., Colberg, J. M., Diaferio, A., & White, S. D. M. 1999, *MNRAS*, 307, 529
- Kravtsov, A. V., Berlind, A. A., Wechsler, R. H., Klypin, A. A., Gottloeber, S., Allgood, B., & Primack, J. R. 2004, *ApJ*, 609, 000 (astro-ph/0308519)
- Landy, S. A., & Szalay, A. S. 1993, *ApJ*, 412, 64
- Magliocchetti, M., & Porciani, C. 2003, *MNRAS*, 346, 186
- Marinoni, C., & Hudson, M. J. 2002, *ApJ*, 569, 101
- Melnick, J., & Sargent, W. L. W. 1977, *ApJ*, 215, 401
- Mo, H. J., & White, S. D. M. 1996, *MNRAS*, 282, 1096
- Moustakas, L. A., & Somerville, R. S. 2002, *ApJ*, 577, 1
- Navarro, J. F., Frenk, C. S., & White, S. D. M. 1995, *MNRAS*, 275, 56
- Navarro, J. F., Frenk, C. S., & White, S. D. M. 1996, *ApJ*, 462, 563
- Navarro, J. F., Frenk, C. S., & White, S. D. M. 1997, *ApJ*, 490, 493
- Netterfield, C. B., et al. 2002, *ApJ*, 571, 604
- Oemler, A. 1974, *ApJ*, 194, 1
- Padilla, N. D., & Baugh, C. M. 2003, *MNRAS*, 343, 796
- Peacock, J. A., & Smith, R. E. 2000, *MNRAS*, 318, 1144
- Pearce, F. R., Jenkins, A., Frenk, C. S., White, S. D. M., Thomas, P. A., Couchman, H. M. P., Peacock, J. A., & Efstathiou, G. 2001, *MNRAS*, 326, 649

- Peebles, P. J. E. 1980, *The Large-Scale Structure of the Universe*, Princeton University Press
- Perlmutter, S., et al. 1999, *ApJ*, 517, 565
- Porciani, C., & Giavalisco, M. 2002, *ApJ*, 565, 24
- Pryke, C., Halverson, N. W., Leitch, E. M., Kovac, J., Carlstrom, J. E., Holzzapfel, W. L., & Dragovan, M. 2001, *ApJ*, 568, 46
- Riess, A. G., et al. 1998, *AJ*, 116, 1009
- Roche, N., Eales, S. A., Hippelein, H., & Willott, C. J. 1999, *MNRAS*, 306, 538
- Roche, N. D., Almaini, O., Dunlop, J., Ivison, R. J., Willott, C. J. 2002, *MNRAS*, 337, 1282
- Roche, N., Dunlop, J., & Almaini, O. 2003, *MNRAS*, 346, 803
- Seljak, U. 2000, *MNRAS*, 318, 203
- Scoccimarro, R., Sheth, R. K., Hui, L., & Jain, B. 2001, *ApJ*, 546, 20
- Sheth, R. K. & Tormen, G. 1999, *MNRAS*, 308, 119
- Sheth, R. K., Hui, L., Diaferio, A., & Scoccimarro, R. 2001, *MNRAS*, 325, 1288
- Sheth, R. K., Mo, H. J., & Tormen, G. 2001, *MNRAS*, 323, 1
- Smith R. E., et al. 2003, *MNRAS*, 341, 1311
- Somerville, R. S., Lemson, G., Sigad, Y., Dekel, A., Kauffmann, G., & White, S. D. M. 2001, *MNRAS*, 320, 289
- Spergel, D. N., et al. 2003, *ApJS*, 148, 175
- Steidel, C. C., Dickinson, M., Giavalisco, M., Pettini, M., Kellogg, M. 1998, *ApJ*, 492, 428
- van den Bosch, Frank, C., Yang, X. H., & Mo, H. J. 2003, *MNRAS*, 340, 77
- Weinberg, D. H., Davé, R., Katz, N., & Hernquist, L. 2004, *ApJ*, 601, 1
- Yang, X. H., Mo, H. J., & van den Bosch, F. C. 2002, *MNRAS*, 339, 1057
- Yoshikawa, K., Taruya, A., Jing, Y. P., & Suto, Y. 2001, *ApJ*, 558, 520
- Zehavi, I., Weinberg, D. H., Zheng, Z., Berlind, A. A., Frieman, J. A., et al. 2004, *ApJ*, 608, 000
(astro-ph/0301280)

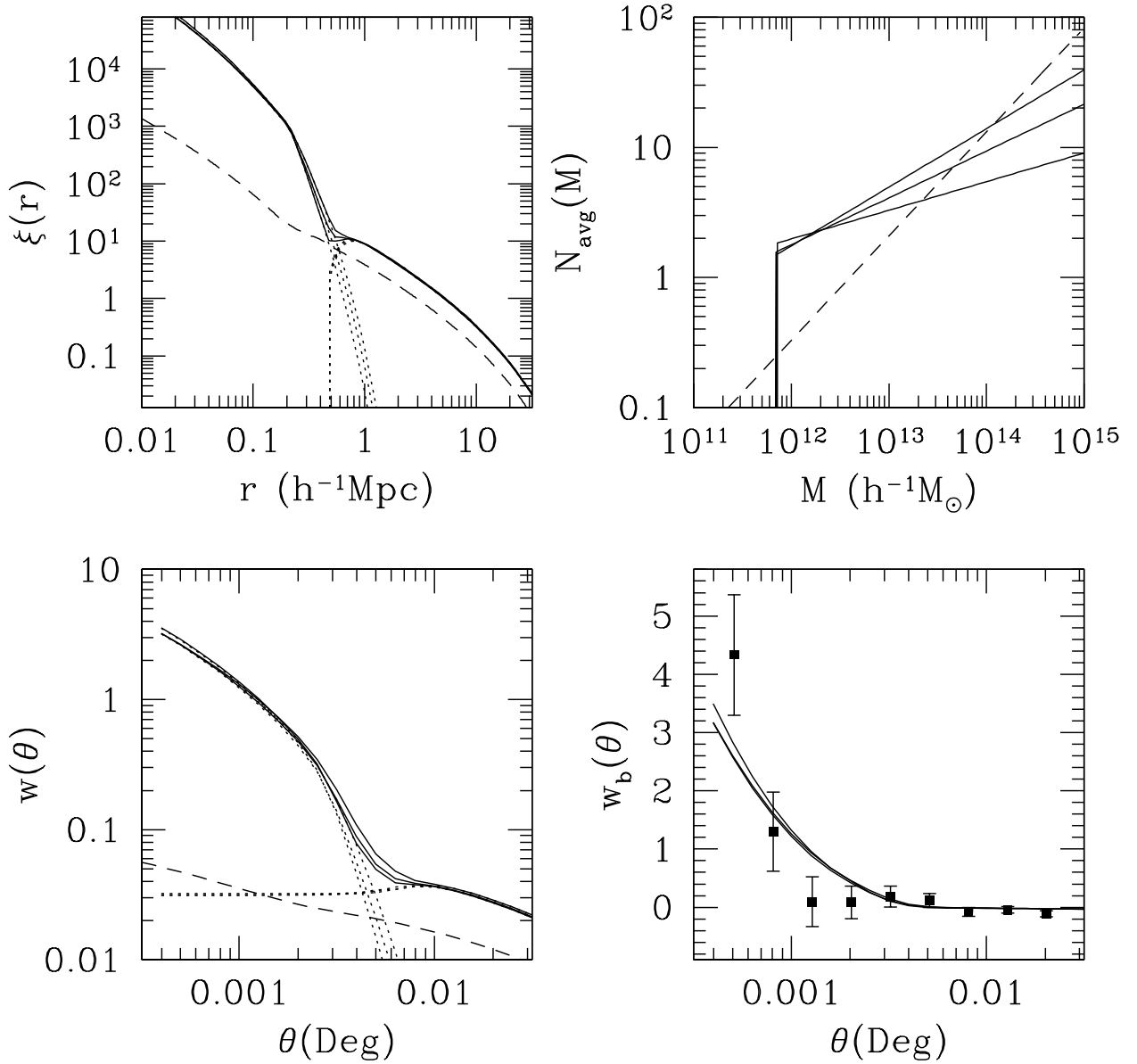


Fig. 1.— Illustration of the loose constraints on individual HOD parameters for the nearest-integer model. Three cases of parameter combinations are shown: $(M_{\min}, M_1, \alpha) = (6.5 \times 10^{11}, 4.5 \times 10^{10}, 0.22)$, $(6.2 \times 10^{11}, 2.0 \times 10^{11}, 0.36)$, and $(6.3 \times 10^{11}, 2.9 \times 10^{11}, 0.45)$, where masses are in units of $h^{-1}M_{\odot}$. The top right panel shows the corresponding mean occupation number as a function of halo mass for the three cases. The top left panel, the bottom left panel, and the bottom right panels are for the real space two-point correlation function, the angular correlation function, and the measured angular correlation function (i.e., with the integral constraint subtracted), respectively. The dotted lines show contributions from one-halo pairs and two-halo pairs. Data points with error bars in the bottom right panel are from Daddi et al. (2003). The dashed line in the top right panel illustrates the mean occupation function of the LBGs, and the dashed curves in the left panels are corresponding correlation functions (see the text).

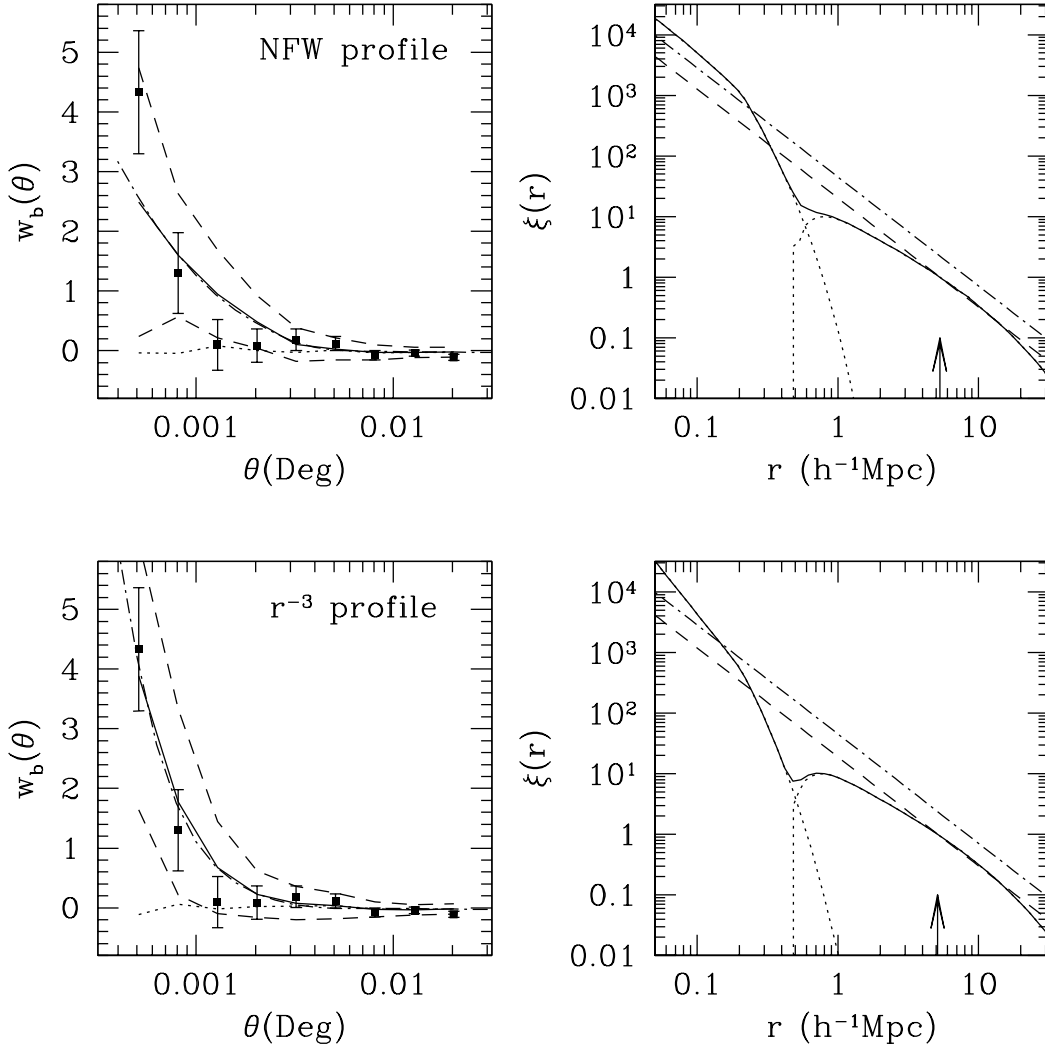


Fig. 2.— Fitting results, sample variance from mock catalogs, and comparison for different assumptions about the galaxy distribution profile within halos. The nearest-integer distribution is used. *Top* : Galaxies distributed according to the NFW profile and $(M_{\min}, M_1, \alpha) = (6.3 \times 10^{11} h^{-1} M_{\odot}, 2.9 \times 10^{11} h^{-1} M_{\odot}, 0.45)$. *Bottom* : Galaxies follow an r^{-3} distribution profile and $(M_{\min}, M_1, \alpha) = (5.8 \times 10^{11} h^{-1} M_{\odot}, 2.7 \times 10^{11} h^{-1} M_{\odot}, 0.38)$. Left panels show the measured angular correlations $w_b(\theta)$. The solid, dashed, and dotted lines are the mean, 1σ scatter about the mean, and the two-halo pair contribution, respectively, measured from mock galaxy catalogs generated through populating $z = 2.97$ halos from the GIF simulation (see the text). The dot-dashed line is the analytic prediction of $w_b(\theta)$. Data points with error bars are from Daddi et al. (2003). The right panels show the corresponding real-space two-point correlation functions. The dotted lines are the one-halo and two-halo terms. Arrows indicate r_0 where $\xi(r_0) = 1$. Two power law curves, $(r/r_0)^{-1.8}$ (*dashed curve*) and $(r/8.3 h^{-1} \text{Mpc})^{-1.8}$ (*dot-dashed curve*), are also plotted for comparison.